Association of Slowly Expanding Lesions on MRI With Disability in People With Secondary Progressive Multiple Sclerosis

Author(s):

Alberto Calvi, MD[1,2]; Ferran Prados Carrasco, PhD[1,3,4]; Carmen Tur, MD, PhD[1,5]; Declan T. Chard, MB, BS, PhD[1,6]; Jonathan Stutters, B.Eng[1]; Floriana De Angelis, MD, PhD[1,5]; Nevin John, MD[1]; Thomas Williams, BA, MB, BChir, MRCP[1]; Anisha Doshi, MD, PhD[1]; Rebecca S Samson, PhD[1]; David MacManus, MSc[1]; Claudia A Gandini Wheeler-Kingshott, PhD[1,7,8]; Olga Ciccarelli, MD, PhD, FRCP[1,6]; Jeremy Chataway, MA, PhD, FRCP[1,6]; Frederik Barkhof, PhD, MD[1,3,6.9] on behalf of the MSSMART Investigators

Corresponding Author:
Alberto Calvi, a.calvi@ucl.ac.uk

Affiliation Information for All Authors: 1. Queen Square MS Centre, Department of Neuroinflammation, Institute of Neurology, Faculty of Brain Sciences, University College London (UCL), United Kingdom; 2. IRCCS Fondazione Ca Granda Ospedale Maggiore Policlinico, University of Milan, Italy; 3. Centre for Medical Image Computing (CMIC), Department of Medical Physics and Biomedical Engineering, University College London, London, United Kingdom; 4. e-Health Centre, Universitat Oberta de Catalunya, Barcelona, Spain; 5. Neurology Department, Luton and Dunstable University Hospital, United Kingdom; 6. National Institute for Health Research, University College London Hospitals, Biomedical Research Centre, London, United Kingdom; 7. Department of Brain and Behavioural Sciences, University of Pavia, Pavia, Italy; 8. Brain Connectivity Centre, IRCCS Mondino Foundation, Pavia, Italy; 9. Radiology & Nuclear medicine, VU University Medical Centre, Amsterdam, The Netherlands.

Equal Author Contribution:

Contributions:
Alberto Calvi: Drafting/revision of the manuscript for content, including medical writing for content; Major role in the acquisition of data; Study concept or design; Analysis or intepretation of data
Ferran Prados Carrasco: Major role in the acquisition of data; Study concept or design; Analysis or intepretation of data
Carmen Tur: Study concept or design; Analysis or intepretation of data; Other
Declan T. Chard: Drafting/revision of the manuscript for content, including medical writing for content; Analysis or intepretation of data
Jonathan Stutters: Major role in the acquisition of data; Analysis or intepretation of data
Floriana De Angelis: Major role in the acquisition of data
Nevin John: Major role in the acquisition of data
Thomas Williams: Major role in the acquisition of data
Anisha Doshi: Major role in the acquisition of data
Rebecca S Samson: Major role in the acquisition of data
David MacManus: Major role in the acquisition of data
Claudia A.M. Gandini Wheeler-Kingshott: Drafting/revision of the manuscript for content, including medical writing for content; Analysis or intepretation of data
Olga Ciccarelli: Drafting/revision of the manuscript for content, including medical writing for content; Study concept or design; Analysis or intepretation of data
Jeremy Chataway: Drafting/revision of the manuscript for content, including medical writing for content; Study concept or design; Analysis or intepretation of data
Frederik Barkhof: Drafting/revision of the manuscript for content, including medical writing for content; Study concept or design; Analysis or intepretation of data

Figure Count:
2

Table Count:
5

Search Terms:
[41] Multiple sclerosis, [130] Volumetric MRI, chronic active lesions, disability, secondary progressive

Handling Editor Statement:

Abstract:

Objectives: To explore the relationship between slowly expanding lesions (SELs) on MRI and disability in secondary progressive multiple sclerosis (SPMS).

Methods: We retrospectively studied 345 patients with SPMS enrolled in the MS-SMART trial (NCT01910259). They underwent brain MRI at baseline, 24 and 96 weeks. Definite SELs were defined as concentrically expanding T2 lesions, as assessed by non-linear deformation of volumetric T1-weighted images. Associations of SEL volumes with other MRI metrics and disability were assessed through Pearson correlations and regression analyses.

Results: Averaged across patients, 29% of T2 lesions were classified as being definite SELs. A greater volume of definite SELs correlated with a higher total baseline T2 lesion volume (r=0.55, p<0.001), and percentage brain volume

reduction (r=-0.26, p<0.001), a higher number of new persisting T1 black holes (r=0.19, p<0.001) and, in a subset of 106 patients, with a greater reduction in magnetization transfer ratio (adjusted difference=0.52, p<0.001). In regression analyses, a higher definite SEL volume was associated with increasing disability, as assessed by the Expanded Disability Status Scale (beta=0.23, p=0.020), z-scores of the Multiple Sclerosis Functional Composite (beta= -0.47, p=0.048), Timed 25 Foot Walk Test (beta= -2.10, p=0.001), Paced Auditory Serial Addition Task (beta= -0.27, p=0.006), and increased risk of disability progression (odds ratio=1.92, p=0.025).

Conclusions: Definite SELs represent almost one third of T2 lesions in SPMS. They are associated with neurodegenerative MRI markers and related to clinical worsening, suggesting that they may contribute to disease progression and be a new target for therapeutic interventions.

Introduction

Recent studies have shown that imaging chronic active (sometimes referred to as "smoldering") lesions may be particularly relevant in progressive multiple sclerosis (MS).[1] Pathologically, they are characterised by the presence of activated peripheral iron-rich macrophages/microglia associated with myelin breakdown,[2,3] reflecting chronic inflammatory activity and incomplete remyelination, and substantial axonal injury. Chronic active lesions are more prevalent in progressive MS phenotypes and are associated with the accrual of disability.[2,4]

On conventional magnetic resonance imaging (MRI), active lesions can be identified when they newly appear (or expand) on T2-weighted scans or show gadolinium-enhancement on T1-weighted scans. [5,6] Such activity is clinically associated with relapses.[7,8] Conversely, persistent T1 hypointense lesions (or black holes) are associated with axonal injury, [9–11] and conventionally thought indicative of the end-stage of lesion evolution.

Chronic active lesions are referred to in histopathological literature as smoldering, slowly expanding, or mixed active-inactive as opposed to the early active, inactive and remyelinated lesions.[12,13] Slowly expanding (or evolving) lesions (SELs) have been proposed as a novel MRI marker of chronic active lesions, and they can be identified using non-rigid longitudinal registration (based on local deformations when aligning consecutive scans) to look for local volume changes in individual lesions.[14] They were initially described in pooled research trials involving relapsing-remitting (RRMS) and primary progressive (PPMS) patients (n=1334, n=555, respectively),[14] with SELs observed in both groups but noticeably more so in PPMS (11.3% vs 8.6% of the total T2 lesion burden). Compared with non-SELs, SELs rarely showed gadolinium enhancement, while T1 intensity within SELs was lower at baseline and showed a greater decrease over time than in non-SELs.[14] In a subsequent study in PPMS patients,[15] a higher T1 lesion volume in SELs predicted clinical progression, thereby suggesting the possibility that SELs could be *in vivo* predictors of axonal loss observed in chronic active lesions.[16]

The aim of this study was to investigate the associations of SELs with physical and cognitive disability scores in secondary progressive MS (SPMS). We also

performed a structural analysis of MTR in order to explore the development of tissue damage within SELs in a subset of patients. We completed our investigation with a descriptive radiological analysis of SELs, including their relationship with other conventional MRI inflammatory and neurodegeneration markers, such as T2 lesion volume change, manually detected new or enlarging T2 lesions, new persistent black holes (PBH), and brain atrophy.

Materials and methods

Participants, clinical assessments and MRI acquisitions. This is a retrospective analysis of 345 SPMS patients who were enrolled in the multi-centre, phase 2b MS-SMART trial (NCT01910259, details reported previously).[17] Inclusion criteria for this study were availability of MRI scans (of sufficient quality for SEL analysis) and clinical assessments at all three time points (baseline, week 24 and week 96). All patients were scanned using 1.5T or 3T MRI scanners at baseline, week 24 and week 96, with the following acquisitions: 3D isotropic T1-weighted (T1); 2D proton density (PD) and T2-weighted (T2); 2D fluid-attenuated inversion recovery (FLAIR).[17] A subset of 106 patients scanned in London and Edinburgh also had 3D MTR imaging at baseline and week 96.[18] Details of the MRI scanners and acquisition parameters are shown in eTable 1 of the Supplementary Materials.

Clinical data included the Expanded Disability Status Scale (EDSS),[19] Symbol Digit Modalities Test (SDMT)[20] and Multiple Sclerosis Functional Composite (MSFC),[21] the latter calculated as the composite of z-scores of the three subcomponents: Nine Hole Peg Test (NHPT), Timed 25 Foot Walk (T25FW)

and Paced Auditory Serial Addition Test (PASAT). Disability progression was defined as a binary outcome by 1-point increase in EDSS (considering the EDSS change from baseline to week-96) if the baseline score was ≤5.0, or a 0.5-point increase if the baseline score was >5.0. [22,23] No assessments were undertaken beyond the 96 weeks of the trial; therefore, it was not possible to evaluate 'confirmed' disability progression.

Standard protocol approvals, registration and patient consents. Written informed consent was obtained for all the participants and the study was approved by the local research ethics committee. Fully anonymized clinical and MRI data were analysed at Queen Square MS Centre, University College London.

T2 lesion segmentation, registration and tissue segmentation. T2 hyperintense lesions were manually identified on the T2/PD/FLAIR baseline images using a semi-automated edge finding tool (JIM v7.0, Xinapse Systems, Aldwincle, UK) and T2 lesion volumes were determined. We defined a participant as a 'MRI outlier' when the total T2 volume was oustide of two standard deviations of the mean, either above or below. New/enlarging T2 lesions were manually identified using a subtraction of the PD/T2 images at baseline and 24/96 weeks. New Persistent black holes (PBH) were similarly manually selected and reported as the number of new T2 lesions at 24 weeks being persistently T1 hypointense at 96 weeks. The original T2 images acquired in 2D with a voxel resolution of (1x1x3) mm^3 were resampled into a 1-mm isotropic space and lesions were co-registered to the 3D-T1 images using a pseudo-T1 image generated by subtracting the PD from the T2-weighted

image;[24] they were then transformed from native space to 3D-T1 space using nearest-neighbour interpolation.

For brain extraction, tissue segmentation and parcellation, Geodesical Information Flows (GIF) was used on the lesion filled 3DT1 scans,[25] providing the following metrics: normalised brain volume (NBV), white matter (WM), cortical grey matter (CGM) and deep grey matter (DGM); lesion-filling was used in this step using a multi-time-point patch-based method to avoid segmentation bias.[26] Percent Brain Volume Change (PBVC) from baseline to week 24 and from baseline to week 96, as measure of brain atrophy, was calculated using the SIENA method.[27]

SEL detection. To identify SELs, we developed an in-house version of the pipeline proposed by Elliot et al.,[28] using a non-linear registration analysis of T2-defined lesions on volumetric T1 images in a two-stage process (SEL detection algorithm). Firstly, 'candidate' SELs were identified from the baseline T2 lesion masks propagated to subsequent scans. A lesion with a positive Jacobian expansion value (JE, i.e., the determinant of the non-linear deformation field) and size of at least 10 mm^3, was classified as a candidate SEL, as per the method of Elliot et al.[14] The remainder of the lesions with a negative JE were classified as non-SELs. The second step identified 'definite' SELs, through a further sub-selection from the candidate SELs. This was based on both the constancy over time and concentricity of their expansion (heuristic score $\geq$0). Constancy was measured by determining the least-squares linear fit of JE over time, taking into account all the intermediate time points. For concentricity, the voxels within each lesion were subdivided into concentric bands from the central core, then mean JE values in each band were plotted against the

distance from the edge, allowing calculation of the slope of the least-squares linear fit. SEL candidates, not satisfying the full two-stage criteria, were designated as 'possible' SELs. We refer to 'SEL-derived volumes' to describe the lesion volumes at baseline. Lesion probability maps (LPM) were obtained separately for definite, possible and non-SELs after registering all subjects to a common MNI anatomical atlas.

Structural analysis of MTR within lesion types. MTR, as percent units (pu), was computed at baseline and week 96, and the difference between baseline and week was also calculated. For each participant the average MTR across all their T2 lesions was calculated. MTR was also analysed at the single lesion level in definite, possible, and non-SELs. To account for registration inaccuracies, MTR values greater or less than two standard deviations from the mean were excluded.

Statistical analysis.

1) Descriptive statistics

Firstly, we evaluated the distribution and the normality assumptions of all the clinical, demographic and MRI variables. Differences in EDSS from baseline to the last follow-up (week 96) were assessed using the Wilcoxon signed-ranked test. Longitudinal changes in clinical scores were calculated by subtracting baseline from week 96 values. Differences in mean T2 lesion volume between baseline and week 96, and changes in mean PBVC between weeks 24 and 96, were compared with changes in PBVC between baseline and week 96 using paired t-tests. Lesion counts were assessd at the patient level by calculating the total number and volume of definite, possible and non-SELs respectively. The

distribution of SEL-derived volumes was positively skewed, and so they were log-transformed (using logartihm on base 10 of the value + 1) to normalise the data.

2) Preliminary analysis of associations between SELs, demographic and other MRI measures

To assess the magnitude and direction of associations Pearson and partial correlations were assessed between log-transformed SEL volumes, other MRI metrics and clinical scores. Simple linear regressions, with log-transformed SEL volumes as predictors and demographic and clinical features (age, sex, disease duration, progression duration, EDSS, MSFC, NHPT, T25FW, PASAT, SDMT) as outcome variables, were performed (eFigure1, Supplementary Materials). Through this association analysis, an evaluation of the relationship between the clinical outcomes and the MRI metrics was carried out with Direct Acyclic Graphs (DAGs) in order to identify confounders to include in the final statistical models (eFigure 2, Supplementary Materials).

3) Association between MTR and SELs

The volumetric and structural MTR analysis was performed at the single lesion level by applying mixed-effects regression models to take into account within subject variability, and they were also adjusted for age, gender and centre (to account for scanner differences).

4) Association between clinical disability outcomes and SELs

Multiple linear regression models were run to explore whether SEL-derived volumes could independently predict disability outcomes. In order to evaluate the added value of SEL-derived volumes when compared with conventional MRI measures, a backward stepwise selection process was undertaken. All models were adjusted for age and sex, T2 lesion volume change and PBVC,

keeping the variables in the models if statistically significant, always forcing age and sex into the models and using a boot-strap approach, including robust standard errors. The final model included the clinical measure at final follow-up (week 96) as the dependent variable, adjusting for the clinical measure at baseline, and the SEL-derived volumes as independent variable, to assess the ability of SEL-derived volumes to predict longitudinal clinical changes. The stability of the final model was confirmed in a forward selection process. In addition, logistic regression models were built to assess the ability of SEL-derived volumes to predict the development of disability progression. All the models residuals were checked for normality. In order to validate the relationship between SEL and the clinical variable measurements across trial time points, repeated-measures mixed-effects models were perfomed, where the dependent variable was the value of the clinical variable (one at a time) at each time point, and the explanatory variables included the time point, SEL-derived volumes, and an interaction term between them. Whenever the interaction terms were significant, we assumed there was a significant association between the clinical variable and the SEL-derived volume, for the time point explored. To take into account for the multicentre structure, all the mixed-effects models were nested at the centre level. Analysis was performed with STATA version 13.1 and all the actual p values were reported.

Data Availability Statement. Fully anonymised data is available after review by the Sponsor (University College London). An application form detailing specific requirements, rationale, and proposed use should be completed, followed by a data-sharing agreement. Requested data may be made available, along with supporting documentation (eg, data dictionary) on a secure server to

appropriate and approved investigators.

Results

Clinical-demographic and conventional MRI metrics. From full MS-SMART trial cohort (n=445), 345 patients fulfilled eligibility criteria. Patients were excluded because of missing scans (n=93) or because the T2 lesion volume was MRI outlier (n=7). Clinical characteristics at baseline and MRI parameters at baseline and follow-up are reported in Table 1. The clinical and radiological characteristics of the patients excluded from the analysis are shown in eTable 2 (Supplementary Materials). No differences between treatment arms were observed in terms of counts and volumes of T2 lesions, or any of the SEL-derived categories (eTable 3, Supplementary Materials). In the retained study cohort, EDSS significantly increased from baseline to the final follow-up (Wilcoxon signed-ranked test, $p<0.001$) and 36.5% of the patients developed disability progression. Mean T2 lesion volume increased significantly from baseline to week 96 (12.54 ml and 12.78 ml, respectively, paired t-test, $p<0.001$). Mean NBV was 1421 ml at baseline, and PBVC from baseline to week 96 was greater than PBVC from week 24 to week 96 (-1.35% and -0.92% respectively, paired t-test, $p<0.001$).

Descriptive analysis of SEL-derived metrics. The descriptive analysis of the lesion types at the patient level is shown in Table 2. 340 of the 345 patients (99%) had at least one definite SEL. The average number of T2 lesions per patient was 67.2, of which 19.5 (29%) were categorised as definite SELs. Mean

T2 lesion volume of definite SELs was 4.4 ml, which accounts for 36% of the overall T2 lesion volume. At the single lesion level, definite SELs were significantly larger than non-SELs (0.25 ml, 95% confidence interval (CI) [0.18 to 0.31] vs 0.14 ml [0.07 to 0.20], respectively, p=0.019 from mixed-effects model to account for within subject variability). The mean annualised change in individual lesion volumes (as determined by the Jacobian values) was 3% (SD 2.9) for definite SELs, 1.5% (SD 3) for possible SELs, and 1.5% (SD 2.2) for non-SELs. Visual inspection of the lesion probability maps revealed no regional differences between definite, possible and non-SELs, although the latter were more prevalent overall (Figure 1).

Association between SEL-derived volumes and conventional MRI metrics.

Significant positive correlations were found between greater definite SEL volume and greater T2 lesion volume change (r=0.24, p<0.001), the number of new/enlarging T2 lesions (manually obtained) at final follow-up (r=0.26, p<0.001), and higher number of new PBHs at final follow-up (r=0.19, p<0.001). A positive correlation was found between definite SEL log-volume and total baseline T2 lesion volume (r=0.55, p<0.001), in partial correlations after accounting for the effect of number of new/enlarging T2 lesions and new PBHs at final follow-up. A higher definite SEL log-volume correlated with higher percentage of brain volume reduction over time (r= -0.26, p<0.001). An example of a patient from this study with a high SEL ratio (relative to total lesion count), worsening of disability and high PBVC is shown in Figure 2.

MTR analysis within SEL-derived lesion types

The mean MTR in definite SELs was significantly lower compared to non-SELs both at baseline and at week 96 (p< 0.001, Table 3). In the longitudinal analysis, the difference between MTR change over time between definite SELs and non-SELs was significant, with a higher rate of MTR reduction from baseline to week 96 was found in the definite SELs when compared with the non-SELs (mixed-effects linear regression models [mean adjusted difference 0.52, 95% CI {0.38 to 0.67}, p<0.001]).

Association between SELs, demographic and clinical features

A higher log-volume of definite SELs at baseline, correlated with higher increase in EDSS over time (Pearson r=0.18, p<0.001). Similarly, when the MSFC and its subtests were analysed, a higher definite SEL log-volume correlated with increasing disability over time, as assessed by changes in the z-scores of the MSFC, T25FW and PASAT (Pearson r ranging from -0.18 to -0.22, p<0.001). No significant associations were found between definite SEL volumes and any of the demographic features assessed (age, sex, disease duration and progression duration).

SELs and clinical disability outcomes at final follow-up:

In stepwise multiple linear regression models, SEL-derived volumes correlated with deterioration of clinical scores at the end of the trial (Table 4). In particular, for each unit increase in definite SEL log-volume (ml), there was a 0.23 (95% CI 0.04 to 0.43) increase in EDSS at follow-up (p=0.020, adjusted R^2=0.56). Similarly, a unit increase in definite SEL log-volume (ml) was associated with a decrease of 0.47 (95% CI -0.98 to -0.03) in MSFC z-score units at follow-up (p=0.048, adjusted R^2=0.38). In both models, T2 volume change and PBVC

were included as covariates. Whereas T2 volume change was not independently associated to change in the clinical measures, PBVC was remained significantly associated with worsening in EDSS and MSFC z-score.

In the logistic regressions, a increase in the definite SEL log-volume was associated with an increased risk of developing disability progression (odds ratio=1.92 [1.08, 3.39], p=0.025, pseudo-R^2=0.03).

The analysis was extended to all the sub-components of the MSFC and the SDMT (Table 4): a increase in the definite SEL log-volume was associated with a worsening of T25FW z-score (beta= -2.10 [-3.43 to -0.85], p=0.001, adjusted R^2=0.20), PASAT z-scores (beta= -0.27 [-0.50 to -0.10], p=0.006, R^2=0.66). Neither non-SEL nor possible SELs log-volumes were significantly associated to any of those clinical scores. No significant associations between all the SEL-derived measures and changes in the NHPT z-score were found. For the SDMT only, increase in non-SEL and possible SEL log-volumes were associated with a worsening in this cognitive score (Table 4).

SELs and longitudinal clinical disability outcomes:

The relationship between SEL volume and longitudinal changes in clinical disability were further confirmed through repeated-measures mixed-effects models across time points (baseline to week 24 and baseline to week 96) adjusted for covariates (age at baseline, sex, total baseline lesion volume, PBVC between baseline and last time point, Table 5). In particular, an association between increased SEL-derived log-volumes and greater worsening in the clinical outcome over time was again found for nearly all the explored measures in the interval from baseline to last time point (week 96). For the EDSS case, the association between SEL-derived volumes and clinical

changes over time could only be confirmed for the first time interval (between baseline and week 24). Regarding SDMT, there was a decrease of the performance from baseline to final time point associated with an increase in all the SEL-derived volumes. The SEL-derived volumes and the other MRI and clinical measures were highly reproducible and not influenced by the study centre, as all the models took into account the multicentre structure (confirmed by intraclass correlation coefficients computation, eTable 4 Supplementary Materials).

Discussion

SELs are a new *in vivo* MRI marker of chronic active lesions which have been recently investigated in RRMS and PPMS cohorts. In this study, for the first time we assessed SELs in a large group of people with SPMS. We found that SEL-derived metrics were associated with more severe lesional damage (as measured by T1 hypointenisty and MTR) and predict physical and cognitive progression in SPMS.

SEL descriptive features

Patients in this cohort had a substantial T2 lesion burden which significantly increased over time, consistent with other clinical trials in SPMS.[29] The descriptive analysis showed that the proportion of patients with at least one SEL was remarkably high (99%), and greater than that observed in PPMS or RRMS (72% and 68%).[30] The mean number of definite SELs (19.5) in the present SPMS cohort was also higher than in PPMS and RRMS (6.3 and 4.6,

respectively).[30] From the total T2 lesion volume per patient the fraction of definite SELs was considerable (36%), indicating that they account for a substantial proportion of lesions. The annualised volume change of definite SELs was on average 3% per year in this SPMS population (previous studies of PPMS and RRMS have not assessed this). Comparsion of our SEL observations in SPMS with those in RRMS suggest that chronic inflammatory activity accumulates over the course of the disease, although differences in techniques may influence the absolute numbers dervied from different studies (as discussed below).

On a lesion-level, definite SELs were significantly bigger than non-SELs. This suggests that there is a greater tendency for on-going lesion expansion in larger lesions, but also may reflect prior lesion enlargement. Previous imaging studies have mainly focused on the spatial location of SELs rather then the morphological or dimensional features. SELs have been described to be preferentially located in the periventicular areas.[30] We also observed this (Figure 1), but noted no difference in lesion distribution between non, possible and definite SELs.

Relationship of SELs with MRI measures of inflammatory and neurodegenerative activity

In a subsample of the MS-SMART study cohort (n=345), we observed a correlation between definite SELs volume and change in overall T2 lesion volume (r=0.24, p<0.001), suggesting that SELs might be a significant contributor to total lesion burden. These findings are in line with pathological studies, where chronic active lesions are asociated with a higher lesion load.[4] In

addition, we found a significant correlation between higher SEL volume and new PBH (r=0.18, p<0.001), in line with previous findings of association of lower and more rapidly decreasing T1 hypointensity within SELs,[15,30] in turn reflecting chronic axonal loss in MS.[9,31] A recent study involving 52 RRMS patients[32] reported a correlation between SELs, normalised brain volume and PBVC (as markers of neurodegeneration), and disability accrual.[33–36] In our study, we extend this observation to SPMS, finding that a higher definite SEL (but not possible or non-SEL) volume was associated with greater brain atrophy (r=-0.26, p<0.001). These results support the hypothesis that SELs contribute significantly to the neurodegenerative process in SPMS.

To further investigate lesion damage, we studied MTR in a subsample of 106 patients, a marker of myelin loss and axonal density reduction histopathologically.[11,37] As expected, MTR within SELs was lower than in non-SELs at baseline. In addition, over time a greater decline in MTR was found in the definite SELs, compared to non-SELs. Similarly, a previous pilot study in RRMS (n=52)[32] found a lower baseline MTR in SELs and an increase in MTR in non-SELs after 24 months follow-up.

SELs correlate with clinical disability

We found a clear association between SELs and disability in SPMS. Elliot et al. previously found that SELs were able to explain 12-week confirmed disability progression as measured by EDSS, and a ≥ 20% increase in T25FW and NHPT in a PPMS trial cohort (n = 732).[15] In our study, we confirm and extend these findings to SPMS, finding that SEL-derived volumes could significantly explain a proportion of EDSS worsening and the development of disability progression

(based on EDSS change from baseline to week 96). Similarly, SEL-derived volumes were associated with worsening of MSFC z-score and an increased odds for disability progression. Interestingly, SEL volumes in isolation explained clinical progression in both the MSFC subcomponents assessing walking and cognitive functions (i.e. T25FW and PASAT), though no significant association with hand function (NHPT) was found. Finally, SDMT worsening, another measure assessing cognitive function, was associated with increases in all the SEL-derived volumes in the mixed-effects models but no associations with the definite SEL volumes were found in the multiple linear regressions.

Methodological considerations

There are some study limitations worth mentioning. SEL analysis can be influenced by many factors, such as image resolution and field strength, the number of time points used, registration and deformation algorithms used, and the definitions (e.g. size, rate of growth) of lesion subtypes. Regarding the SEL definition, we applied a volume threshold of 10 mm^3 as per Elliot et al.,[28] recognising that the computation of non-linear deformations in smaller spatial areas reduces reliability. However, in contrast to Elliot et al., we did not threshold lesions based on rates of expansion. Also in contrast to Elliot et al.,[30] we did not try to disentangle confluent lesions as, on careful review of such lesions, we could not distinctly separate merging lesions.

Post-contrast T1-weighted scans were not available in this study, so we could not assess the relationship between SEL and contrast-enhanced lesions. However, in SPMS the frequency of gadolinium enhancing lesions is low (10% as reported in SPMS trials)[22] and a previous study showed that contrast-enhancement is not a common feature of SELs.[30]

The magnitude associations and effect sizes in our analyses were for some extent small or borderline significant. However, given the nature of this exploratory study, analysing the impact of a novel MRI marker, any sign of association to the disability measures, even if weak, has been considered valuable.

100 patients had to be excluded due to incompatibility with the inclusion criteria (i.e. missed MRI scans) not allowing to perform the SEL analysis with our pipeline. However, the robustness of the results of the multiple linear regression including the clinical outcome variables has been accounted for by using a multiple imputation model for the missing data (eTable 5, Supplementary Materials). Moreover, an added value of the SEL pipeline used in this study is that is highly reproducible across centres, using common pipelines and conventional MRI sequences (PD/T2-weighted and T1-weighted).

Future developments and alternative imaging markers in SPMS

To date, SELs have been observed over periods of 2-3 years, but it is not clear if SELs remain active perpetually or eventually become quiescent as they have not been investigated yet over longer time period. In contrast to SELs, there is also evidence that over decades some lesions may also shrink or even disappear.[38,39] In addition to the T1 and MTR signature, other microstructural and cellular properties of SELs could be studied, using advanced quantitative MRI or targeted PET techniques, providing greater insights into the pathobiology of SELs. The presence of a lesion rim on susceptibility-weighted MRI has been proposed as an alternative imaging marker for chronic active MS lesions, [40–42] albeit also imperfect [43], but it is unclear how these relate to SELs. Interestingly, retrospective volumetric analysis has provided evidence that rim-

positive lesions have a tendency to expand.[3,44] As with SELs, a higher number of rim-positive lesoins appears to be associated with clinical severity,[45] and peristence of rim-postive lesions is associated with a worse prognosis,[44] although the temporal dynamics of rims appearance and persistence are not entirely clear. Furthermore, using quantitative susceptibility mapping (QSM), as with SELs, hyperintese rims appear to be more common in progressive MS, and in patients with higher levels of disability.[46]

In conclusion, SELs are a common feature in SPMS, and make up a substantial fraction of the T2 lesion volume. They correlate with other markers of neurodegeneration and relate to disability progression. As a marker of ongoing (smouldering) activity in the absence of overt new activity, they may shed light on currently elusive mechanisms of progression, and represent a target for anti-inflammatory treatments behind a closed blood-brain barrier.[47]

Table 1. Demographic, clinical, and radiological characteristics of the patients whose scans contributed to the SEL study

Demographics and clinical metrics	Number of patients	345
	Age, median [y] (IQR)	55.9 (50.0 – 60.4)
	Female n (%)	230 (67%)
	Baseline disease duration, median [y] (IQR)	21 (15 – 22)
	Baseline progression duration, median [y] (IQR)	6 (3 – 8)
	Number of patients allocated to the treatment arms, n (% total): − Fluoxetine − Riluzole − Amiloride − Placebo	90 (26.1%) 85 (24.6%) 86 (24.9%) 84 (24.4%)
	EDSS at baseline, median (IQR)	6.0 (5.5 – 6.5)
	EDSS change from baseline to week 96, mean (SD)	0.11 (0.72)
	Patients with disability progression over time, number (%)	126 (37%)
	MSFC z-score at baseline, mean (SD)	-0.02 (0.85)
	MSFC z-score change, mean (SD)	-0.41 (1.40)
	NHPT at baseline, mean [sec^{-1}] (SD)	0.03 (0.01)
	NHPT z-score change, mean (SD)	-0.12 (0.58)
	T25FW at baseline, mean [sec] (IQR)	11.2 (8.2 – 17.5)
	T25FW z-score change, mean (SD)	-1.17 (3.86)
	PASAT score at baseline, mean (SD)	38.8 (14.9)
	PASAT z-score change, mean (SD)	0.09 (0.69)
	SDMT score at baseline, mean (SD)	44.4 (12.5)
	SDMT change, mean (SD)	0.58 (7.13)
MRI metrics	T2 lesion volume at baseline, mean [ml] (SD)	12.54 (10.85)
	T2 lesion volume at week 96, mean [ml] (SD)	12.78 (10.99)
	New/enlarging T2 lesions at week 96, mean number (SD)	2.67 (6.23)
	New PBH at week 96, mean number (SD)	0.32 (1.14)
	NBV at baseline, mean [ml] (SD)	1421 (85)
	CGM at baseline, mean [ml] (SD)	790 (44)
	DGM at baseline, mean [ml] (SD)	45 (4)
	WM at baseline, mean [ml] (SD)	588 (44)
	PBVC, mean [%] (SD) − week 24 to week 96 − baseline to week 96	 -0.94 (1.20) -1.35 (1.27)

Abbreviations: IQR=interquartile range; SD=standard deviation; EDSS=expanded disability status scale; MSFC=multiple sclerosis functional composite; NHPT=nine-hole peg test; T25FW=timed 25-foot walk test; PASAT=paced auditory serial addition task; SDMT=symbol digit modalities test; PBH=persistent black holes (manually detected); NBV=normalised brain volume; CGM=cortical grey matter volume; DGM=deep grey matter

volume; WM=white matter volume; PBVC=percent brain volume change. All the changes in the clinical metrics were calculated as the difference between the week 96 and the baseline relative values.

Table 2. SEL-derived metrics at the patient level (n= 345)

Lesion type		Number of lesions per patient, mean (range)	Ratio to total T2 lesions	Lesion volume per patient, mean [ml] (range)	Ratio to total T2 lesion volume
T2 lesion		67.2 (3 – 352)	NA	12.3 (0.1 – 71.4)	NA
SEL category	non-SEL	41.2 (1 – 284)	0.61	5.6 (0.1 – 37.7)	0.46
	possible SEL	6.4 (0 – 36)	0.10	2.3 (0 – 38.8)	0.18
	definite SEL	19.5 (0 – 94)	0.29	4.4 (0 – 39.7)	0.36

Total T2 lesions, and then lesion measures for each SEL category. The ratio to total T2 lesions is the number of lesions in a given SEL-derived category relative to the total number of lesions.

Table 3. Magnetization Transfer Ratio (MTR) at baseline and 96 weeks follow-up, and MTR changes over time in the different lesion types.

T2 Lesion types	MTR in individual lesions (n=6,938)			
	MTR baseline*, pu	MTR week 96*, pu	MTR change*	p value
non SEL **(n= 4395)**	29.77 (29.22 – 30.32)	30.03 (29.47 – 30.58)	0.26 (0.14, 0.37)	**p<0.001**
possible SEL **(n= 659)**	27.91 (27.27 – 28.54)	27.80 (27.17 – 28.43)	-0.11 (-0.40, 0.18)	p=0.351
definite SEL **(n= 1884)**	28.77 (29.20 – 29.34)	28.50 (27.93 – 29.07)	-0.27 (-0.44, -0.10)	**p=0.002**

*Data from 6,938 T2 lesions, presented as adjusted mean (95% confidence intervals) obtained from the mixed-effects model (covariates included were age, gender and site). Bold indicateds significant results (p-value <0.05).

Table 4. Multiple linear/logistic regressions between SEL-associated log-volumes and clinical scores.

	Non SEL log-volume beta or OR (95% CI) * p value	Possible SEL log-volume beta or OR (95% CI) * p value	Definite SEL log-volume beta or OR (95% CI) * p value
EDSS	beta=-0.04(-0.25,0.16), p=0.695	beta=0.07 (-0.12, 0.27), p=0.461	beta=**0.23 (0.04, 0.43), p=0.020**
MSFC z-score	beta=-0.04(-0.37,0.28), p=0.809	beta=-0.24 (-0.79, 0.18), p=0.323	beta=**-0.47 (-0.98, -0.03) p=0.048**
NHPT z-score	beta=-0.12(-0.31,0.06), p=0.180	beta=-0.13 (-0.31, 0.03), p=0.127	beta=-0.09 (-0.28, 0.08), p=0.313
T25FW z-score	beta=-0.53(-1.42,0.40), p=0.263	beta=-0.69 (-2.19, 0.69), p=0.340	beta=**-2.10 (-3.43, -0.85), p=0.001**
PASAT z-score	beta=-0.06(-0.25,0.12), p=0.533	beta=-0.18 (-0.37, 0.01), p=0.056	beta=**-0.27 (-0.50, -0.10), p=0.006**
SDMT	beta=**-3.02(-5.18, -1.12) p=0.004**	beta=**-2.77 (-5.05, -0.22), p=0.026**	beta=-2.06 (-4.08, 0.29), p=0.067
Disability progression	OR=0.84 (0.47, 1.48), p=0.537	OR=1.43 (0.75, 2.71), p=0.276	OR=**1.92 (1.08, 3.39), p=0.025**

*Regression coefficients (beta) or odds ratio (OR) and 95% confidence intervals (95% CI) of linear/logistic regressions performed with the SEL-derived metrics as predictors (definite SEL, possible SEL and non-SEL log-volumes) and the clinical measure (at baseline and week 96) as response variable, therefore representing the change in the clinical measure explained by the SEL-derived metrics. All models were adjusted for age, gender, and T2 lesion volume change and percentage brain volume change (when those metrics were contributing to the models). In bold the significant results set as p-value <0.05.

Abbreviations: beta=regression coefficient; OR=odds ratio; 95% CI=confidence interval; EDSS=Expanded Disability Status Scale; MSFC=Multiple Sclerosis Functional Composite; NHPT= Nine-Hole Peg Test, T25FW=Timed 25-Foot Walk Test; PASAT=Paced Auditory Serial Addition Task; SDMT=Symbol Digit Modalities Test.

Table 5. Association between SEL-derived volumes and clinical outcomes over

time using mixed-effects regression models

Explanatory variables (below)	Dependent variable, interaction term: beta (95%CI), p-value		
	Non SEL log-volume	**Possible SEL log-volume**	**Definite SEL log-volume**
EDSS change baseline – wk24 baseline – wk96	-0.04 (-0.21,0.13), p=0.647 0.02 (-0.14,0.19), p=0.775	0.11 (-0.09,0.31), p=0.274 0.01 (-0.19,0.21), p=0.938	**0.30 (0.13,0.47), p=0.001** -0.07 (-0.24,0.10), p=0.431
MSFC z-score change baseline – wk24 baseline – wk96	0.01(-0.31,0.33), p=0.961 -0.15 (-0.47,0.18), p=0.375	-0.12 (-0.50,0.25), p=0.519 -0.25 (-0.63,0.12), p=0.185	-0.14 (-0.46,0.19), p=0.405 **-0.80 (-1.13,-0.48), p<0.001**
NHPT z-score change baseline – wk24 baseline – wk96	-0.06 (-0.20,0.08), p=0.433 -0.13 (-0.28,0.01), p=0.065	0.02 (-0.14,0.19), p=0.776 -0.11 (-0.27,0.05), p=0.184	-0.01 (-0.14,0.14), p=0.995 -0.13 (-0.28,0.01), p=0.075
T25FW z-score baseline – wk24 baseline – wk96	0.16 (-0.72,1.05), p=0.716 -0.30 (-1.19,0.59), p=0.504	-0.51 (-1.54,0.51), p=0.327 -0.59 (-1.62,0.44), p=0.265	-0.59 (-1.48,0.31), p=0.199 **-2.02 (-2.91,-1.13), p<0.001**
PASAT z-score baseline – wk24 baseline – wk96	-0.10 (-0.29,0.08), p=0.269 -0.01 (-0.19,0.18), p=0.964	0.12 (-0.09,0.33), p=0.269 -0.07 (-0.29,0.14), p=0.502	0.06 (-0.13,0.24), p=0.548 **-0.31 (-0.49,-0.12), p=0.001**
SDMT change baseline – wk24 baseline – wk96	-0.88 (-2.78,1.01), p=0.364 **-2.47 (-4.37,-0.57), p=0.011**	-1.00 (-3.27,1.28), p=0.390 **-2.51 (-4.83,-0.20), p=0.033**	-1.19 (-3.13,0.74), p=0.226 **-2.63 (-4.59,-0.67), p=0.009**

The table shows the interaction terms between time point and SEL-derived log-
volumes. Whenever the interaction term is significant, we assume that there is a
significant association between the SEL-derived log-volumes and the change in the
clinical variable over time. All the models are adjusted for sex, baseline T2 lesion
volume and PBVC. In bold the significant results set as p-value <0.05.

Figure 1. Lesion probability maps (LPM)

From left to right, lesion probability maps for definite, possible and non-SELs. Red indicates a lower probability (starting at 3%) and yellow a higher one (bigger than 10%).
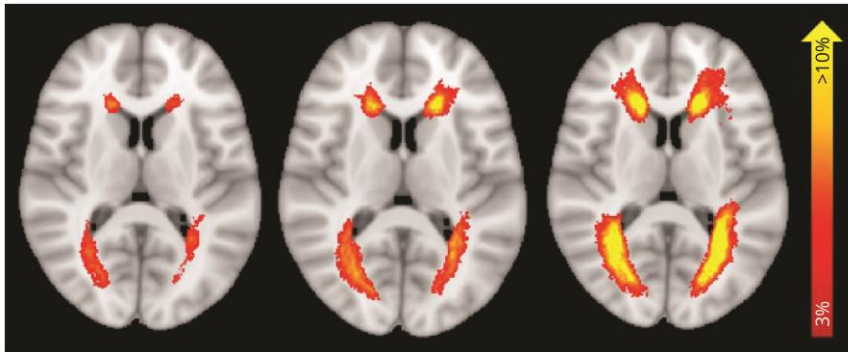
Figure 2. Example of patient with high number of SELs

From left to right: T1 at baseline, T1 at week 96 and registered T1 with Jacobian maps overlayed (red color refers to prevalence of positive Jacobian values of expansion, while blue color is related to volume stability). Out of 27 total T2 lesions identified, 16 were definite SELs (59%). EDSS at baseline was 5.5 and EDSS at week 96 was 8. Percent brain volume change from baseline to week 96 was -2.5%.

WNL-2022-200397_coinvestigator_appendix --http://links.lww.com/WNL/B868

WNL-2022-200397_sup -- http://links.lww.com/WNL/B869
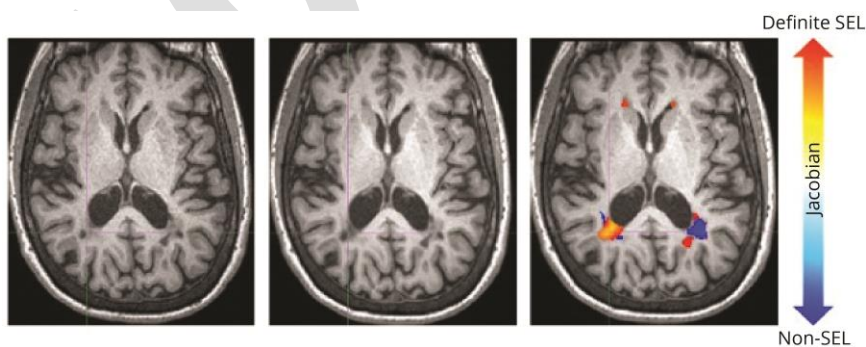
References

1. Calvi A, Haider L, Prados F, Tur C, Chard D, Barkhof F. In vivo imaging of chronic active lesions in multiple sclerosis. *Mult Scler J*. September 2020:135245852095858. doi:10.1177/1352458520958589
2. Frischer JM, Weigand SD, Guo Y, et al. Clinical and pathological insights into the dynamic nature of the white matter multiple sclerosis plaque. *Ann Neurol*. 2015;78(5):710-721. doi:10.1002/ana.24497
3. Dal-Bianco A, Grabner G, Kronnerwetter C, et al. Slow expansion of multiple sclerosis iron rim lesions: pathology and 7 T magnetic resonance imaging. *Acta Neuropathol*. 2017;133(1):25-42. doi:10.1007/s00401-016-1636-z
4. Luchetti S, Fransen NL, van Eden CG, Ramaglia V, Mason M, Huitinga I. Progressive multiple sclerosis patients show substantial lesion activity that correlates with clinical disease severity and sex: a retrospective autopsy cohort analysis. *Acta Neuropathol*. 2018;135(4):511-528. doi:10.1007/s00401-018-1818-y
5. Brück W, Bitsch A, Kolenda H, Brück Y, Stiefel M, Lassmann H. Inflammatory central nervous system demyelination: Correlation of magnetic resonance imaging findings with lesion pathology. *Ann Neurol*. 1997. doi:10.1002/ana.410420515
6. Tan IL, van Schijndel RA, Fazekas F, et al. Image registration and subtraction to detect active T 2 lesions in MS: an interobserver study. *J Neurol*. 2002;249(6):767-773. doi:10.1007/s00415-002-0712-6
7. Sormani MP, Bruzzi P. MRI lesions as a surrogate for relapses in multiple sclerosis: A meta-analysis of randomised trials. *Lancet Neurol*. 2013;12(7):669-676. doi:10.1016/S1474-4422(13)70103-0
8. Fisniku LK, Brex PA, Altmann DR, et al. Disability and T2 MRI lesions: A 20-year follow-up of patients with relapse onset of multiple sclerosis. *Brain*. 2008;131(3):808-817. doi:10.1093/brain/awm329
9. Van Walderveen MAA, Lycklama à Nijeholt GJ, Adér HJ, et al. Hypointense lesions on T1-weighted spin-echo magnetic resonance imaging: Relation to clinical characteristics in subgroups of patients with multiple sclerosis. *Arch Neurol*. 2001;58(1):76-81. doi:10.1001/archneur.58.1.76
10. Van Waesberghe JHTM, Kamphorst W, De Groot CJA, et al. Axonal loss in multiple sclerosis lesions: Magnetic resonance imaging insights into substrates of disability. *Ann Neurol*. 1999;46(5):747-754. doi:10.1002/1531-8249(199911)46:5<747::AID-ANA10>3.0.CO;2-4
11. Schmierer K, Scaravilli F, Altmann DR, Barker GJ, Miller DH. Magnetization transfer ratio and myelin in postmortem multiple sclerosis brain. *Ann Neurol*. 2004;56(3):407-415. doi:10.1002/ana.20202
12. Kuhlmann T, Ludwin S, Prat A, Antel J, Brück W, Lassmann H. An updated histological classification system for multiple sclerosis lesions.

   Acta Neuropathol. 2017;133:13-24. doi:10.1007/s00401-016-1653-y

13. Frischer JM, Bramow S, Dal-Bianco A, et al. The relation between inflammation and neurodegeneration in multiple sclerosis brains. *Brain*. 2009;132(5):1175-1189. doi:10.1093/brain/awp070

14. Elliott C, Wolinsky J, Hauser J, et al. Detection and characterisation of slowly evolving lesions in multiple sclerosis using conventional brain MRI. *Mult Scler J*. 2017;23(3_suppl):52. doi:10.1177/1352458517731283

15. Elliott C, Belachew S, Wolinsky JS, et al. Chronic white matter lesion activity predicts clinical progression in primary progressive multiple sclerosis. *Brain*. 2019;142(9):2787-2799. doi:10.1093/brain/awz212

16. Frischer JM, Bramow S, Dal-Bianco A, et al. The relation between inflammation and neurodegeneration in multiple sclerosis brains. *Brain*. 2009;132(5):1175-1189. doi:10.1093/brain/awp070

17. Chataway J, De Angelis F, Connick P, et al. Efficacy of three neuroprotective drugs in secondary progressive multiple sclerosis (MS-SMART): a phase 2b, multiarm, double-blind, randomised placebo-controlled trial. *Lancet Neurol*. 2020;19(3):214-225. doi:10.1016/S1474-4422(19)30485-5

18. Samson RS, Cardoso MJ, Muhlert N, et al. Investigation of outer cortical magnetisation transfer ratio abnormalities in multiple sclerosis clinical subgroups. *Mult Scler J*. 2014;20(10):1322-1330. doi:10.1177/1352458514522537

19. Kurtzke JF. Rating neurologic impairment in multiple sclerosis: An expanded disability status scale (EDSS). *Neurology*. 1983;33(11):1444-1444. doi:10.1212/WNL.33.11.1444

20. Smith A. The Symbol-Digit Modalities Test: A neuropsychologic test for economic screening of learning and other cerebral disorders. *Learn Disord*. 1968;3:83-91.

21. Cutter GR, Baier ML, Rudick RA, et al. Development of a multiple sclerosis functional composite as a clinical trial outcome measure. *Brain*. 1999;122(5):871-882. doi:10.1093/brain/122.5.871

22. Kappos L, Bar-Or A, Cree BAC, et al. *Siponimod versus Placebo in Secondary Progressive Multiple Sclerosis (EXPAND): A Double-Blind, Randomised, Phase 3 Study*. Vol 391.; 2018. doi:10.1016/S0140-6736(18)30475-6

23. Lublin F, Miller DH, Freedman MS, et al. *Oral Fingolimod in Primary Progressive Multiple Sclerosis (INFORMS): A Phase 3, Randomised, Double-Blind, Placebo-Controlled Trial*. Vol 387.; 2016. doi:10.1016/S0140-6736(15)01314-8

24. Hickman SJ, Barker GJ, Molyneux PD, Miller DH. Technical note: The comparison of hypointense lesions from "pseudo-T1" and T1-weighted images in secondary progressive multiple sclerosis. *Mult Scler*. 2002;8(5):433-435. doi:10.1191/1352458502ms824xx

25. Cardoso MJ, Modat M, Wolz R, et al. Geodesic Information Flows: Spatially-Variant Graphs and Their Application to Segmentation and Fusion. *IEEE Trans Med Imaging*. 2015;34(9):1976-1988. doi:10.1109/TMI.2015.2418298

26. Prados F, Cardoso MJ, Kanber B, et al. A multi-time-point modality-agnostic patch-based method for lesion filling in multiple sclerosis. *Neuroimage*. 2016;139:376-384. doi:10.1016/j.neuroimage.2016.06.053

27. Smith SM, Zhang Y, Jenkinson M, et al. Accurate, robust, and automated

longitudinal and cross-sectional brain change analysis. *Neuroimage.* 2002;17(1):479-489. doi:10.1006/nimg.2002.1040

28. C. Elliott, J.S. Wolinsky, S.L. Hauser, L. Kappos, F. Barkhof, C. Bernasconi, S. Belachew, Arnold D. Detection and characterisation of slowly evolving lesions in multiple sclerosis using conventional brain MRI. In: *ECTRIMS Online Library. Elliott C. Oct 27 2017; 202544.* ; 2017:53. https://onlinelibrary.ectrims-congress.eu/ectrims/2017/ACTRIMS-ECTRIMS2017/202544/colm.elliott.detection.and.characterisation.of.slowly.evolving.lesions.in.html.

29. Tur C, Moccia M, Barkhof F, et al. Assessing treatment outcomes in multiple sclerosis trials and in the clinical setting. *Nat Rev Neurol.* 2018;14(2):75-93. doi:10.1038/nrneurol.2017.171

30. Elliott C, Wolinsky JS, Hauser SL, et al. Slowly expanding/evolving lesions as a magnetic resonance imaging marker of chronic active multiple sclerosis lesions. *Mult Scler J.* 2019;25(14):1915-1925. doi:10.1177/1352458518814117

31. Van Waesberghe JHTM, Kamphorst W, De Groot CJA, et al. Axonal loss in multiple sclerosis lesions: Magnetic resonance imaging insights into substrates of disability. *Ann Neurol.* 1999;46(5):747-754. doi:10.1002/1531-8249(199911)46:5<747::AID-ANA10>3.0.CO;2-4

32. Preziosa P, Pagani E, Moiola L, Rodegher M, Filippi M, Rocca MA. Occurrence and microstructural features of slowly expanding lesions on fingolimod or natalizumab treatment in multiple sclerosis. *Mult Scler J.* 2020. doi:10.1177/1352458520969105

33. Truyen L, Van Waesberghe JHTM, Van Walderveen MAA, et al. Accumulation of hypointense lesions ('black holes') on T1 spin-echo MRI correlates with disease progression in multiple sclerosis. *Neurology.* 1996;47(6):1469-1476. doi:10.1212/WNL.47.6.1469

34. Giorgio A, Stromillo ML, Bartolozzi ML, et al. Relevance of hypointense brain MRI lesions for long-term worsening of clinical disability in relapsing multiple sclerosis. *Mult Scler.* 2014;20(2):214-219. doi:10.1177/1352458513494490

35. Radue EW, Barkhof F, Kappos L, et al. Correlation between brain volume loss and clinical and MRI outcomes in multiple sclerosis. *Neurology.* 2015;84(8):784-793. doi:10.1212/WNL.0000000000001281

36. De Stefano N, Giorgio A, Battaglini M, et al. Assessing brain atrophy rates in a large population of untreated multiple sclerosis subtypes. *Neurology.* 2010;74(23):1868-1876. doi:10.1212/WNL.0b013e3181e24136

37. Van Waesberghe JHTM, Kamphorst W, De Groot CJA, et al. Axonal loss in multiple sclerosis lesions: Magnetic resonance imaging insights into substrates of disability. *Ann Neurol.* 1999;46(5):747-754. doi:10.1002/1531-8249(199911)46:5<747::AID-ANA10>3.0.CO;2-4

38. Sethi V, Nair G, Absinta M, et al. Slowly eroding lesions in multiple sclerosis. *Mult Scler J.* 2016:464-472. doi:10.1177/1352458516655403

39. Pongratz V, Schmidt P, Bussas M, et al. Prognostic value of white matter lesion shrinking in early multiple sclerosis: An intuitive or naïve notion? *Brain Behav.* 2019;9(12). doi:10.1002/brb3.1417

40. Bagnato F, Hametner S, Yao B, et al. Tracking iron in multiple sclerosis: a combined imaging and histopathological study at 7 Tesla. *Brain.* 2011;134(12):3602-3615. doi:10.1093/brain/awr278

41. Wisnieff C, Ramanan S, Olesik J, Gauthier S, Wang Y, Pitt D.

Quantitative susceptibility mapping (QSM) of white matter multiple sclerosis lesions: Interpreting positive susceptibility and the presence of iron. *Magn Reson Med.* 2015;74(2):564-570. doi:10.1002/mrm.25420

42. Yao B, Bagnato F, Matsuura E, et al. Chronic multiple sclerosis lesions: Characterization with high-field-strength MR imaging. *Radiology.* 2012. doi:10.1148/radiol.11110601

43. Popescu BF, Frischer JM, Webb SM, et al. Pathogenic implications of distinct patterns of iron and zinc in chronic MS lesions. *Acta Neuropathol.* 2017;134(1):45-64. doi:10.1007/s00401-017-1696-8

44. Absinta M, Sati P, Schindler M, et al. Persistent 7-tesla phase rim predicts poor outcome in new multiple sclerosis patient lesions. *J Clin Invest.* 2016;126(7):2597-2609. doi:10.1172/JCI86198

45. Absinta M, Sati P, Masuzzo F, et al. Association of Chronic Active Multiple Sclerosis Lesions With Disability In Vivo. *JAMA Neurol.* August 2019. doi:10.1001/jamaneurol.2019.2399

46. Harrison DM, Li X, Liu H, et al. Lesion heterogeneity on high-field susceptibility MRI Is associated with multiple sclerosis severity. *Am J Neuroradiol.* 2016;37(8):1447-1453. doi:10.3174/ajnr.A4726

47. Lassmann H. Targets of therapy in progressive MS. *Mult Scler.* 2017;23(12):1593-1599. doi:10.1177/1352458517729455